

# Halo and Tail Generation Study in Compact Linear Collider

I. Ahmed <sup>1</sup>, H. Burkhardt <sup>2</sup>, M. Fitterer

<sup>1</sup> National Centre for Physics (NCP), Islamabad, Pakistan

<sup>2</sup> European Organizations for Nuclear Research (CERN), Geneva, Switzerland

<sup>3</sup> Universitat Karlsruhe, Germany

Email contact of main author: ijaz.ahmed@cern.ch

**Abstract.** Halo particles in linear colliders can result in significant losses and serious background which may reduce the overall performance. We discuss halo sources and describe analytical estimates. We report about generic halo and tail simulations and estimates. Previous studies were mainly focused on very high energies as relevant for the beam delivery systems of linear colliders. We have now studied, applied and extended these simulations to lower energies as relevant for the CLIC drive beam.

## 1. Introduction

Halo particles contribute very little to the luminosity but may instead be a major source of background and radiation [1]. Even if most of the halo will be stopped by collimators, the secondary muon background may still be significant [2, 3].

We study halo production with detailed simulations, to accompany the design studies for future linear colliders such that any performance limitations due to halo and tails can be minimised [4].

One of our aims was to assemble a comprehensive list of potential halo production processes. We find it useful to subdivide this list in three categories.

Particle processes:

- Beam Gas elastic scattering and multiple scattering
- Beam Gas inelastic scattering, bremsstrahlung
- Synchrotron radiation, incoherent and coherent
- Scattering off thermal photons
- Intrabeam and Touschek scattering
- Ion or electron-cloud effects

Optics related:

- Mismatch
- Coupling
- Dispersion
- Non-linearities

Collective and equipment related:

- Wake-fields
- Beam Loading
- Noise and vibration
- Dark currents
- Space charge effects close to source
- Bunch compressors

This list was presented and discussed at several conferences including EPAC'06 [4] and PAC'07 [5] and in various EuroTeV meetings. It can be considered as a rather complete, agreed basis.

The first category of halo production processes we have considered are the particle scattering processes. The importance of particle scattering processes in the production of halo particles was observed in storage rings. In LEP in particular, a good agreement between the observed halo and expectations from particle scattering processes was observed under stable running conditions [6].

Beam gas scattering is the most basic and in many cases the dominant halo generating particle process. We provide a full simulation of both elastic and inelastic scattering on the HTGEN generator level [7] as well as analytical estimates, both of which will further be described below.

Halo particles which hit aperture limits like the beam pipe or collimators are normally not followed up, but rather counted as lost and optionally written to output files which can be used as input to cascade simulation codes like GEANT [8]. For thin objects like spoilers instead, we provide the possibility to simulate multiple scattering and energy loss and to continue tracking. The halo generator code package HTGEN includes generic interface routines to facilitate integration in tracking codes. Specific interfaces have been made for the PLACET [9] and MERLIN [10] programs. Synchrotron radiation is included in the tracking programs and has been further optimised [11].

Our analytical estimates show, that halo from scattering off thermal photons does not exist at low energies and will still be rather negligible at high energy linear colliders. A simulation code for the scattering off thermal photons is described in [12].

Intrabeam and Touschek scattering can be rather important at low energies in the damping ring. The simulation of these processes is currently outside the scope of this study. Ion or electron-cloud effects can result on local heating and vacuum increase. The simulation of these effects is rather specific and followed as separate tasks. The results in terms of vacuum increase can be fed back into the simulations considered here by modification of the input parameters for beam gas scattering.

In addition to particle scattering processes, optics related effects like mismatch, coupling, dispersion and non-linearities can enhance the beam halo. This is studied by combining the halo generation with detailed tracking programs and also allows studying the effect of wake fields, alignment and ground motion on the core and halo of the beam. The Monte Carlo halo generator code for the particle scattering processes is provided as program package HTGEN [7]. The package includes documentation, installation instructions, standalone test procedures for each process as well as interface routines for the PLACET and MERLIN programs.

### **Elastic scattering**

In the elastic process of Mott scattering, the incident beam particle is deflected by the Coulomb potential of the particles in the residual gas. Elastic scattering changes the direction of the beam particle while its energy is not affected. Elastic scattering can lead to large betatron amplitudes and loss of particles at collimators or any other aperture restriction.

The angular distribution of the scattered electron is given by the differential Mott cross section [13]

$$\frac{d\sigma}{d\Omega} = \left[ \frac{Zr_e}{2\gamma\beta^2} \right]^2 \frac{1 - \beta^2 \sin^2 \frac{\theta}{2}}{\sin^4 \frac{\theta}{2}},$$

where  $Z$  is the charge of the nucleus,  $r_e$  the classical electron radius and  $\gamma$  the Lorentz factor  $E/mc^2$  of the electron. Note that  $\beta$  is here the velocity in units of the speed of light. For a

simple estimate, we use  $\beta = 1$ ,  $\sin(\vartheta/2) \sim \vartheta/2$  and see that the angular distribution is dominated by the Coulomb term  $16/\theta^4$ .

The total cross section is obtained by integration over the solid angle. Relevant for halo production are scattering angles which exceed the beam divergence, or roughly

$$\theta_{\min} = \sqrt{\frac{\varepsilon}{\beta_y}} = \sqrt{\frac{\varepsilon_N}{\gamma\beta_y}}$$

where  $\varepsilon_N = \gamma\varepsilon$  is the normalized vertical emittance and  $\beta_y$  the local vertical beta function. After integration, we can use the same small angle approximation as above to get as a simple estimate for the integrated elastic cross section as a function of the minimum scattering angle

$$\sigma_{el} = \frac{4\pi Z^2 r_e^2}{\gamma^2 \theta_{\min}^2}$$

Using Eq. 2 we can rewrite the cross section in terms of the normalized emittances [14] as

$$\sigma_{el} = \frac{4\pi Z^2 r_e^2 \beta_y}{\gamma \varepsilon_N}$$

At constant normalized emittance, the elastic cross section scales inversely with energy.

### Inelastic scattering

At high energy, the dominating process relevant for energy loss or inelastic scattering is bremsstrahlung in which the incident electron interacts with the field of the residual gas nucleus and radiates a photon. The energy spectrum is rather broad and can be approximately written as

$$\frac{d\sigma}{dk} = \frac{A}{N_A X_0} \frac{1}{k} \left( \frac{4}{3} - \frac{4}{3}k + k^2, \right)$$

where  $k$  is the photon energy in units of the beam energy,  $N_A$  the Avogadro constant,  $X_0$  and  $A$  are the radiation length and the mass of the material. Integration over  $k$  (from  $k = k_{\min}$  to  $k = 1$ ) yields

$$\sigma_{in} = \frac{A}{N_A X_0} \left( -\frac{4}{3} \log k_{\min} - \frac{5}{6} + \frac{4}{3} k_{\min} - \frac{k_{\min}^2}{2} \right)$$

The cross section does not vary with energy at fixed  $k_{\min}$ . For  $k = k_{\min} = 0.01$  the inelastic cross section is 0.375 barn per Helium Atom and 6.510 barn for N2 for the sum of the two nuclei. The angular cross section is given by

$$f(\theta)d\theta \propto \frac{\theta d\theta}{(\theta^2 + \gamma^{-2})^2}.$$

### CLIC Drive Beam Decelerator

The CLIC Drive Beam decelerator will extract X-band RF power from a 100 A Drive Beam. The focussing and alignment systems must ensure transport of particles of all energies through the decelerator sectors, ensuring minimal losses. A short summary of relevant beam parameters is given in Table 1 and a more detailed description can be found in [4].

Table 1: CLIC drive beam decelerator parameters

Parameter	Unit	Value
Drive beam sector length	m	1053
numb. of part. per bunch	$10^9$	52.5
numb. of bunches per train		2928
mean initial beam energy	GeV	2.40
mean final beam energy	GeV	0.40

$\epsilon_{N,y,initial}$	$\mu\text{m}$	150.0
$\epsilon_{N,y,final}$	$\mu\text{m}$	334

## DISCUSSION FOR THE CLIC DECELERATOR

### Analytical Estimates

We expect to have the largest halo generation in the longest decelerator, for which we performed the simulations. For the analytical estimates of beam gas scattering and Compton scattering we assumed a residual gas constitution of 40%  $\text{H}_2\text{O}$ , 40%  $\text{H}_2$  and the remaining 20% shared among  $\text{CO}$ ,  $\text{N}_2$ ,  $\text{CO}_2$ , a pressure of 10 nTorr and a temperature of 300 K. As minimal scattering angle  $\theta_{\min}$  we used the beam divergence and as minimal photon energy with respect to the beam energy  $k_{\min} = 0.01$ . The beam divergence and the beam energy were calculated from the simulation results. We based our calculations for Compton scattering on [10]. The results are presented in Table 2. Elastic scattering is the dominant process and increases along the beamline. The energy spread caused by Compton scattering stays below 0.25% and is negligible compared to the energy spread due to the deceleration of the beam. The total scattering probability integrated over the whole decelerator is  $7.69 \cdot 10^{-9}$ . Therefore we expect very little halo generation due to beam gas and Compton scattering. The cross sections for beam gas scattering change slightly,

Table 2: Analytical estimates for beam-gas scattering and Compton scattering.  $\rho$  is the molecule density in the case of beam gas scattering and the photon density in the case of Compton scattering,  $P_{\text{init}}$  and  $P_{\text{final}}$  the initial and final scattering probability.

Process	$\rho[\text{m}^{-3}]$	$P_{\text{init}}[\text{m}^{-1}]$	$P_{\text{final}}[\text{m}^{-1}]$
Mott	$3.22 \cdot 10^{14}$	$7.96 \cdot 10^{-12}$	$4.21 \cdot 10^{-11}$
Brems.	$3.22 \cdot 10^{14}$	$1.11 \cdot 10^{-13}$	$1.11 \cdot 10^{-13}$
Comp.	$5.45 \cdot 10^{14}$	$3.63 \cdot 10^{-14}$	$3.63 \cdot 10^{-14}$

When the effect of ionization of the residual gas is taken into account. Our analytical estimates show that the ionization level stays below 3%, so no extension of our model is required.

The total number of intra-beam-scattering events per unit time scales with  $1/\beta^4$  [11], where  $\beta$  is the velocity in units of speed of light, and increases with the particle density, which shows that intrabeam scattering as well as Touschek effect become more relevant for low energy beams with a small beam size. In the CLIC decelerator the Touschek effect could be more important than in comparable linear accelerators without decelerating sections, because beam particles, which have performed Touschek scattering and lost longitudinal momentum, could lose almost all their longitudinal momentum during the deceleration and get lost.

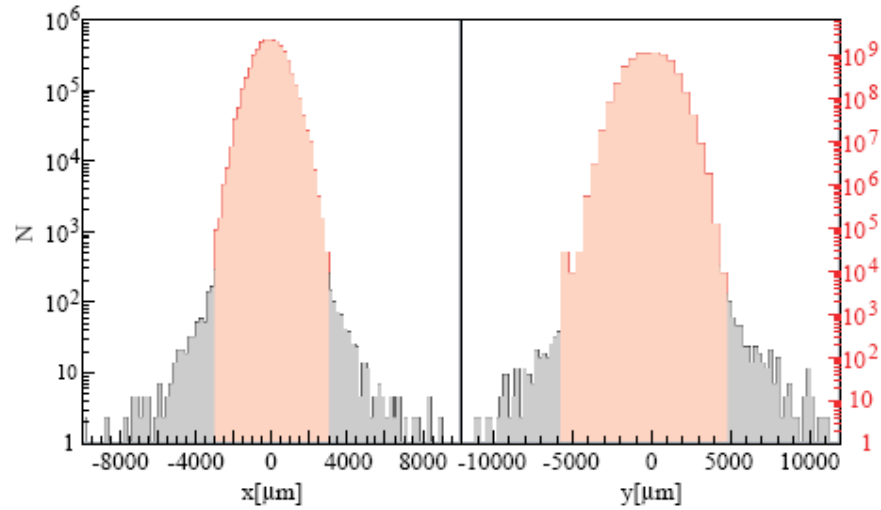
As the drive beam is a negatively charged beam, only ion cloud effects are important. Ion cloud effects are known from ring accelerators, but also in linear accelerators instability can occur - the fast ion instability. We have performed analogous analytical studies for the decelerator as for the CLIC long transfer lines [12]. To ensure the stability of the beam, the number of rise-times should stay below one. Taking the initial beam parameters it lies between 1.9 and 5.7 and taking the final beam parameters between 0.5 and 1.6, which might indicate an eventual appearance of the fast ion instability.

### Simulation Results

In the simulations we used a sliced beam model with a reduced number of bunches per train. We included alignment errors as well as an initial beam offset in the vertical and horizontal plane. For simplicity we performed the simulation with a gas equivalent consisting of pure nitrogen. Our tracking results are shown in Fig. 1 and Fig. 2. If the amplitude of a particle

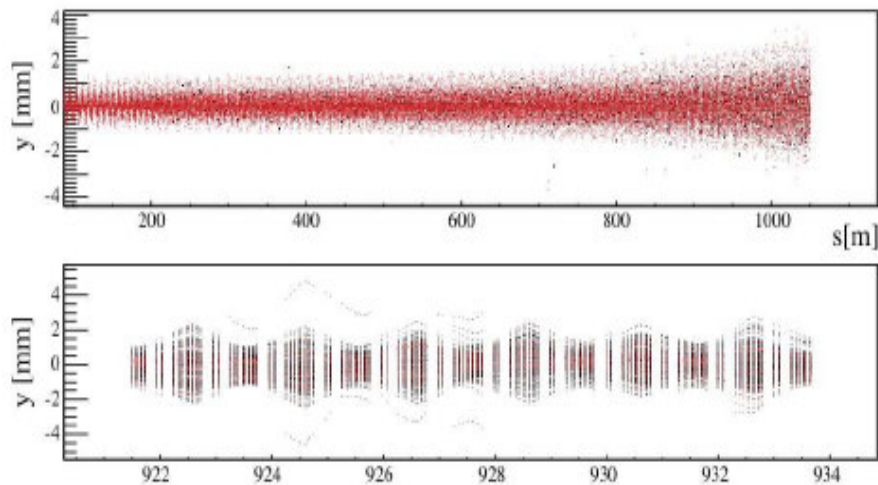
exceeds the aperture of the element it is considered as lost. We find that only a very small fraction of  $10^{-7}$  particles

Figure 1: Transverse Beam profiles at the exit of the CLIC



is lost. Most of these are low energy particles with large scattering angles, which are lost at the end of the beamline.

Figure 2: Vertical beam position along the complete CLIC decelerator and along an extract. Halo particles are shown in black, beam particles in red



### CTF3 Drive Beam Decelerator

The CLIC test facility will demonstrate the essential parts of the CLIC drive beam generation scheme consisting of a fully loaded linac, a delay loop and a combiner ring [13]. The final CLIC Test Facility (CTF3) drive beam delivered to the CLIC Experimental Area (CLEX) comprising the test beam line and a two beam test stand, has an energy of 150 MeV, 35 A of beam current, a bunch repetition frequency of 15 GHz and a pulse length of 140 ns. Main differences between the CTF3 beam and the CLIC drive beam are the energy and the current. The aim of Transfer Beam Line (TBL) is to extract as much energy as possible out of the beam and to demonstrate the stability of the decelerated beam and the produced rf power. The main issues are the transport of a beam with a very high energy spread with no significant beam loss

and suppression of the wake fields from the Power Extraction and Transfer Structures (PETS). Finally TBL will produce RF power in the GW range which could be used to test several accelerating structures in parallel. Since last decade the increasing interest for high-intensity, high-energy linear accelerators have induced the scientific community to consider a phenomenon whose effects are worrying: the beam losses. Lost particles can, indeed, produce complicated problems in operation and maintenance of the machine. Usually such kind of particles originate in a low density particles called halo which can extend far from the beam core and are small fraction of beam particles. Analytical estimates are undertaken in order to understand the physics of halo production and to develop methods to limit and control beam losses. The previous study was performed mainly for high energy beam for beam delivery system for linear colliders.

An analytical estimate for elastic beam-gas scattering is calculated for a constant normalized emittance of 150 mrad at  $\beta_y = 3.40164$  m.  $\rho$  is the density of nitrogen gas molecules per cubic meter and  $P$  the scattering probability per electron per meter over the CTF3-TBL, we find that an electron has a probability of about  $3.37 \times 10^{-10}$  per meter to produce halo particles to undergo elastic scattering with an angle of at least the beam divergence equal to 329 mrad. The probability integrated over the CTF3-TBL is about  $7.41 \times 10^{-9}$ . In the simulation, the beam gas temperature, pressure and other parameters are shown in Table 3.

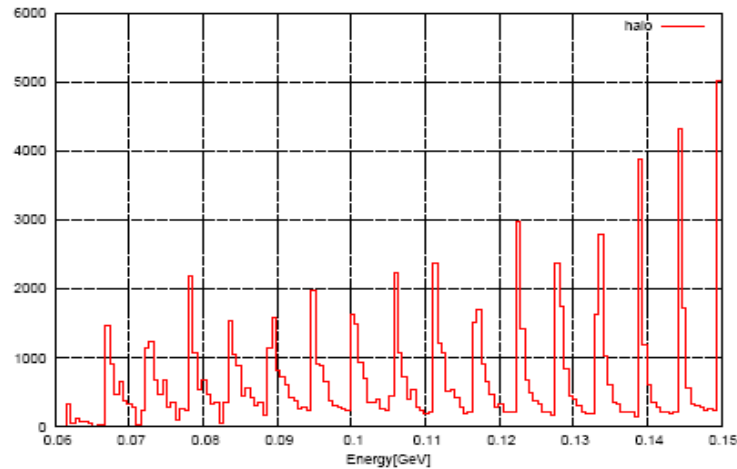
Table 3: Few beam parameters are shown.

CTF3-TBL length [m]	21.99
Z mean ( $N_2$ )	7
Pressure [nTorr]	10
Temperature [K]	300
Npart	$4 \times 10^9$
Particle density [ $10^{14} \text{m}^{-3}$ ]	6.438
$K_{\min}$	0.01

The simulations described here were performed for an ideal machine without errors and positioning tolerances. For the nominal intensity of  $1.4575 \times 10^{10}$  particles per bunch and 200 bunches in TBL, we expect that  $2.16 \times 10^4$  particles are scattered and named as halo particles, in each train crossing. Similarly for the case of CLIC drive beam, with particle intensity of  $5.25 \times 10^{10}$  per bunch and 50 bunches in train will produce  $3.15 \times 10^6$  halo per train.

Figures 3 show the deceleration of the halo particles through the TBL after passing through successive decelerating structures. The decelerating structures are assumed to have one longitudinal and one transverse mode. Each of these two modes can be described by a loss factor, a wavelength, a group velocity and a damping. The PETS model includes single and multi bunch effect. The monopole field is used to decelerate while the set of dipole modes gives kick on the transverse plane.

Figure 3: This plot demonstrates the deceleration of halo particles.



### SUMMARY AND OUTLOOK

We have extended the simulation capabilities of PLACET-HTGEN to low energy, high intensity beams, performed simulations for the CLIC drive beam decelerator and presented the results together with analytical estimates. We have started to apply PLACET-HTGEN to the Test Beam Line drive beam [4] and intend to perform simulations for other low energy linear accelerators like for example TBone [14]. To provide an even more complete simulation of low energy beams, we consider including also a simple model of the Touschek effect. An extension of the fast-ion simulation code FASTION [15] for the CLIC drive beam is in progress.

### REFERENCES

- [1] H. Burkhardt, L. Neukermans, "Halo and Tail generator package HTGEN" <http://hbu.home.cern.ch/hbu/HTGEN.html>.
- [2] A. Latina, E. Adli, H. Burkhardt, Y. Renier, G. Rumolo, D. Schulte, R. Tomas, "Recent Improvements in the Tracking Code PLACET", EUROTeV-Report-2008-043
- [3] H. Burkhardt, L. Neukermans, A. Latina, D. Schulte, I. Agapov, G.A. Blair, F. Jackson, "Halo Estimates and Simulations for Linear Colliders", PAC'07, Albuquerque, New Mexico, USA, WEOCC03, p. 2041
- [4] E. Adli et. al, "Beam Dynamics of the CLIC Decelerator", To be published in proceedings of the X-Band RF Structure and Beam Dynamics Workshop 2008, The Cockcroft Institute, United Kingdom
- [5] B. Povh, K. Rith, Ch. Scholz, F. Zetsche, "Particles and Nuclei", Springer, 1999, edition 4
- [6] Y. Tsai, "Pair production and Bremsstrahlung of charged leptons", Review of Modern Physics, Oktober 1974, Rev.Mod.Phys. 46, p. 815-851
- [7] Particle Data Group, "Passage of particles through matter", Review of Particle Physics, 2008
- [8] S.T. Perkins, D.E. Cullen, S.M. Seltzer, "EEDL", UCRL-50400, 1991, vol. 31
- [9] Geant 4, "Physics Reference Manuel", December 2008, p. 120-134
- [10] V.I. Telnov, "Scattering of electrons on thermal radiation photons in electron-positron storage rings", Nucl. Inst. Meth., 1987, vol. A260, p. 304-308
- [11] A. Piwinski, "The Touschek Effect in Strong Focusing Storage Rings", DESY, 98-179, November 1998
- [12] J.B. Jeanneret, E. Adli, A. Latina, G. Rumolo, D. Schulte, R. Tomas, "Beam Dynamics Issues in the CLIC Long Transfer Lines", EPAC'08, Genoa, Italy, 2008, THPC018, p. 3017
- [13] G. Geschonke and A. Ghigo, "CTF3 Design Report", CERN/PS 2002-008 and LNF-02/008, 2002.

- [14] A.-S. Muller et al., "Ultra-fast High-Power Coherent THz to Mid-IR Radiation Facility", PAC'09, Vancouver, Canada, 2009, TU5RFP028
- [15] G. Rumolo, D. Schulte, "Fast Ion Instability in the CLIC Transfer Line and Main Linac", EPAC'08, Genoa, Italy, 2008, MOPP048, p. 655